

# Controlled soliton formation in tailored Bessel photonic lattices

Falko Diebel,<sup>1,\*</sup> Martin Boguslawski,<sup>1</sup> Tigran Dadalyan,<sup>2</sup>  
Rafael Drampyan,<sup>2</sup> and Cornelia Denz<sup>1</sup>

<sup>1</sup>*Institut für Angewandte Physik and Center for Nonlinear Science (CeNoS), Westfälische Wilhelms-Universität Münster, 48149 Münster, Germany*

<sup>2</sup>*Institute for Physical Research, National Academy of Sciences of Armenia, 0203, Ashtarak, Armenia*

[\\*falko.diebel@uni-muenster.de](mailto:falko.diebel@uni-muenster.de)

**Abstract:** Azimuthally modulated higher order rotationally symmetric Bessel-like optical patterns were generated by coherent superposition of two co-propagating Bessel beams – either in or out of phase. By changing the distance between the beam centers, a whole variety of transition states can be realized. As one prominent example, a 4-fold symmetry quadrupole-like photonic structure was optically inducted in an SBN crystal and nonlinear beam propagation in such a photonic wave-guiding structure is investigated in both self-focusing and self-defocusing regimes. The proposed device serves as an all-optical 2d  $1 \times 4$  photonic interconnect.

© 2016 Optical Society of America

**OCIS codes:** (190.4420) Nonlinear optics, transverse effects in; (190.6135) Spatial solitons; (350.5500) Propagation; (190.5330) Photorefractive optics; (140.3300) Laser beam shaping.

---

## References and links

1. S. Trillo and W. Torruellas, *Spatial Solitons* (Springer Series in Optical Sciences, 2001).
2. F. Lederer, G. I. Stegeman, D. N. Christodoulides, G. Assanto, M. Segev, and Y. Silberberg, “Discrete solitons in optics,” *Phys. Rep.* **463**, 1–126 (2008).
3. Y. S. Kivshar and G. P. Agrawal, *Optical Solitons: From Fibers to Photonic Crystals* (Academic Press, 2003).
4. D. N. Neshev, E. Ostrovskaya, Y. S. Kivshar, and W. Krolikowski, “Spatial solitons in optically induced gratings,” *Opt. Lett.* **28**, 710–712 (2003).
5. J. W. Fleischer, M. Segev, N. K. Efremidis, and D. N. Christodoulides, “Observation of two-dimensional discrete solitons in optically induced nonlinear photonic lattices,” *Nature* **422**, 147–150 (2003).
6. B. Terhalle, A. S. Desyatnikov, C. Bersch, D. Träger, L. Tang, J. Imbrock, Y. S. Kivshar, and C. Denz, “Anisotropic photonic lattices and discrete solitons in photorefractive media,” *Appl. Phys. B* **86**, 399–405 (2007).
7. J. Xavier, M. Boguslawski, P. Rose, J. Joseph, and C. Denz, “Reconfigurable optically induced quasicrystallographic three-dimensional complex nonlinear photonic lattice structures,” *Adv. Mater.* **22**, 356–360 (2010).
8. J. Durnin, J. J. Miceli, and J. H. Eberly, “Diffraction-free beams,” *Phys. Rev. Lett.* **58**, 1499–1501 (1987).
9. F. P. Schäfer, “On some properties of axicons,” *Appl. Phys. B* **39**, 1–8 (1986).
10. J. Turunen, A. Vasara, and A. T. Friberg, “Holographic generation of diffraction-free beams,” *Appl. Opt.* **27**, 3959–3962 (1988).
11. N. Chattrapibhan, E. A. Rogers, D. Cofield, W. T. Hill, and R. Roy, “Generation of nondiffracting Bessel beams by use of a spatial light modulator,” *Opt. Lett.* **28**, 2183–2185 (2003).
12. A. Badalyan, R. Hovsepyan, P. Mantashyan, V. Mekhitarian, and R. Drampyan, “Bessel standing wave technique for optical induction of complex refractive lattice structures in photorefractive materials,” *J. Mod. Opt.* **60**, 617–628 (2013).
13. P. Rose, M. Boguslawski, and C. Denz, “Nonlinear lattice structures based on families of complex nondiffracting beams,” *New J. Phys.* **14**, 033018 (2012).
14. R. Fischer, D. N. Neshev, S. Lopez-Aguayo, A. S. Desyatnikov, A. A. Sukhorukov, W. Krolikowski, and Y. S. Kivshar, “Observation of light localization in modulated Bessel optical lattices,” *Opt. Express* **14**, 2825–2830 (2006).

15. P. Rose, F. Diebel, M. Boguslawski, and C. Denz, "Airy beam induced optical routing," *Appl. Phys. Lett.* **102**, 101101 (2013).
16. F. Diebel, B. M. Bokić, M. Boguslawski, A. Piper, D. V. Timotijević, D. M. Jović, and C. Denz, "Control of Airy-beam self-acceleration by photonic lattices," *Phys. Rev. A* **90**, 033802 (2014).
17. K. Staliunas, R. Herrero, C. Cojocar, and J. Trull, "Nondiffractive propagation of light in photonic crystals," in *Proceedings of the 7th International Conference on Transparent Optical Networks, Ict.* **1**, 281–283 (2005).
18. Y. V. Kartashov, A. A. Egorov, V. A. Vysloukh, and L. Torner, "Stable soliton complexes and azimuthal switching in modulated Bessel optical lattices," *Phys. Rev. E* **70**, 065602 (2004).
19. Y. V. Kartashov, A. A. Egorov, V. A. Vysloukh, and L. Torner, "Rotary dipole-mode solitons in Bessel optical lattices," *J. Opt. B Quantum Semiclass. Opt.* **6**, 444–447 (2004).
20. Y. V. Kartashov, R. Carretero-Gonzalez, B. A. Malomed, V. A. Vysloukh, and L. Torner, "Multipole-mode solitons in Bessel optical lattices," *Opt. Express* **13**, 10703–10710 (2005).
21. Y. V. Kartashov, V. A. Vysloukh, and L. Torner, "Stable ring-profile vortex solitons in Bessel optical lattices," *Phys. Rev. Lett.* **94**, 043902 (2005).
22. D. Song, C. Lou, L. Tang, X. Wang, W. Li, X. Chen, K. J. H. Law, H. Susanto, P. G. Kevrekidis, J. Xu, and Z. Chen, "Self-trapping of optical vortices in waveguide lattices with a self-defocusing nonlinearity," *Opt. Express* **16**, 10110–10116 (2008).
23. X. Wang, Z. Chen, and P. G. Kevrekidis, "Observation of discrete solitons and soliton rotation in optically induced periodic ring lattices," *Phys. Rev. Lett.* **96**, 083904 (2006).
24. S. Huang, P. Zhang, X. Wang, and Z. Chen, "Observation of soliton interaction and planetlike orbiting in Bessel-like photonic lattices," *Opt. Lett.* **35**, 2284 (2010).
25. K. Buse, U. van Stevendaal, R. Pankrath, and E. Kratzig, "Light-induced charge transport properties of  $\text{Sr}_{0.61}\text{Ba}_{0.39}\text{Nb}_2\text{O}_6:\text{Ce}$  crystals," *J. Opt. Soc. Am. B* **13**, 1461 (1996).
26. A. A. Zozulya and D. Z. Anderson, "Propagation of an optical beam in a photorefractive medium in the presence of a photogalvanic nonlinearity or an externally applied electric field," *Phys. Rev. A* **51**, 1520 (1995).
27. T. I. Lakoba and J. Yang, "A generalized Petviashvili iteration method for scalar and vector Hamiltonian equations with arbitrary form of nonlinearity," *J. Comput. Phys.* **226**, 1668–1692 (2007).
28. J. C. Gutierrez-Vega, M. Iturbe-Castillo, G. Ramirez, E. Tepichin, R. M. Rodriguez-Dagnino, S. Chavez-Cerda, and G. New, "Experimental demonstration of optical Mathieu beams," *Opt. Commun.* **195**, 35–40 (2001).
29. F. Diebel, D. Leykam, M. Boguslawski, P. Rose, C. Denz, and A. S. Desyatnikov, "All-optical switching in optically induced nonlinear waveguide couplers," *Appl. Phys. Lett.* **104**, 261111 (2014).
30. J. C. Gutiérrez-Vega, M. Iturbe-Castillo, and S. Chávez-Cerda, "Alternative formulation for invariant optical fields: Mathieu beams," *Opt. Lett.* **25**, 1493–1495 (2000).

## 1. Introduction

Soliton formation in nonlinear media is one of the most interesting nonlinear processes for both, their fundamentals and for numerous potential applications. In nonlinear materials the spreading of spatially localized optical beams during propagation (due to diffraction) can be compensated by nonlinear self-focusing. If exactly balanced, the resulting self-channeled beams, known as "spatial optical solitons," are highly robust which make them very promising objects for control and guiding approaches. In the past, spatial solitons in homogeneous nonlinear medium have been studied in numerous works [1].

The presence of photonic lattices – micro-metric scale refractive index modulations – provides a powerful way to guide and control solitons and their dynamics. The soliton behavior now is fundamentally different from that in a uniform medium and still a challenging topic in modern optics. In periodic nonlinear lattices self-focusing or self-defocusing characteristics of the medium can balance the lattice diffraction, resulting in discrete lattice solitons [2].

The desired periodic refractive index modulation can be pre-fabricated in photonic crystals [3] or optically induced in photorefractive materials [4–7]. The illumination of a photorefractive medium with intensity-modulated light leads to a corresponding change in the refractive index. The advantage of this optical induction method is the possibility to gain high nonlinear response at very low power levels, as well as the flexibility to record different refractive index structures reversibly. Many important experimental works in this field successfully used these features of photorefractive strontium barium niobate (SBN) crystals [4–6].

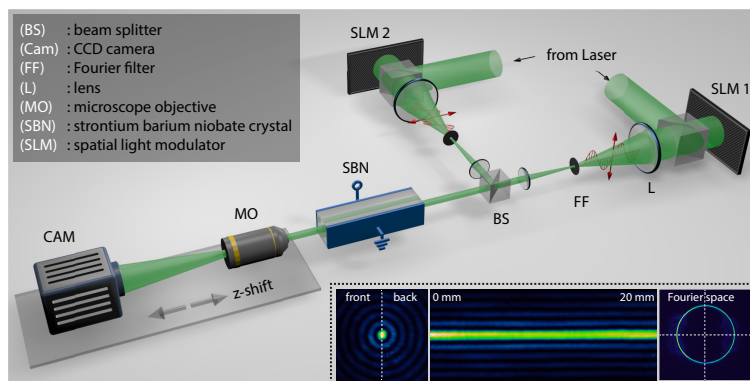


Fig. 1. Experimental setup and Bessel beam characterization. The inset shows the experimentally realized single Bessel beam at the front and back face of the homogeneous SBN crystal, as well as a cross-section through the recorded 3d intensity volume and the spatial spectrum in Fourier space.

If considering two-dimensional structures, nondiffracting beams are of special interest for optical induction because they enable the realization of non-spreading high-contrast structures due to the feature of unchanged propagation in free space [8]. One fundamental example for nondiffracting beams are Bessel beams, having a radial intensity distribution expressed by the Bessel function of first kind. They can for example be generated by axicons [9], computer generated holograms [10], and spatial light modulators [11]. Combined with its counter-propagating part, Bessel standing wave provides a radial and axial modulation that can be used to optically induce three-dimensionally modulated photonic structures [12]. Other nondiffracting beams such as discrete beams, higher-order Bessel, Weber, or Mathieu beams [13] have been realized and successfully used to optically induce corresponding 2d photonic lattices. The generation of higher order azimuthally modulated Bessel lattices by employing a phase imprinting technique was reported in [14]. Moreover, accelerated beams, such as Airy beams, have been used to optically induce an all-optical router [15] and even controlled with photonic lattices [16]. On the other hand, particular periodic refractive index modulations are found to result in a nondiffractive propagation of light as described in [17].

In the last decade, there was an increasing interest in soliton formation in Bessel structures and many novel effects of self-trapping multipole-mode solitons [18–20] and vortex solitons [21, 22] in self-focusing and self-defocusing media have been predicted and observed. Also rotary solitons and planet-like orbiting of solitons in Bessel-like photonic lattices were demonstrated [23, 24].

In this paper, we introduce an inventive approach to create a whole variety of different nondiffracting beams resulting from the coherent superposition of two transversely shifted zero-order Bessel beams. Thereby, the addressable variety of structures range from simple azimuthally modulated to complex Mathieu-like structures depending on the transverse displacement and the phase relation between the two Bessel beams. For one representative configuration, a four-fold modulated Bessel-like optical beam, we perform the optical induction in photorefractive SBN and demonstrate the light guiding potential in both regimes – focusing and defocusing. Finally, we study the nonlinear soliton formation in this quadrupole-like structure by performing the transition from linear wave guiding to nonlinear localization.

## 2. Experimental setup and approach

The experimental setup is shown schematically in Fig. 1. The light from a cw laser at a wavelength of 532 nm is split into two beams, one serves as induction beam, the other as probe beam. The ordinarily polarized induction beam is modulated by a phase-only spatial light modulator (SLM 1) in combination with two following lenses and the Fourier filter in the focal plane. In a similar way, the extraordinary probe beam is shaped with SLM 2. A beam splitter directly in front of the nonlinear crystal combines both beams. As nonlinear medium we use a 20 mm long cerium doped  $\text{Sr}_{0.60}\text{Ba}_{0.40}\text{Nb}_2\text{O}_6$  (SBN:Ce) crystal externally biased by an electric field of  $E_{\text{ext}} = \pm 1.5 \text{ kV cm}^{-1}$  applied along the c-axis (the sign of  $E_{\text{ext}}$  determines whether the nonlinearity is self-focusing or self-defocusing). The doping with cerium was found to significantly enhance the photorefractive properties of SBN [25].

The illumination of photorefractive crystals by inhomogeneous light redistributes charge carriers excited by photoionization, builds up an internal electric fields and in this way changes the refractive index via the electro-optic effect, thus allowing the induction of photonic refractive index structures. Depending on the polarization of the light, the refractive index change for ordinary and extraordinary beams is determined by  $\Delta n_o = -1/2n_{o,0}^3 r_{13} E_{\text{ext}}$  and  $\Delta n_e = -1/2n_{e,0}^3 r_{33} E_{\text{ext}}$ , respectively, where  $r_{13} = 47 \text{ pm V}^{-1}$  and  $r_{33} = 237 \text{ pm V}^{-1}$  are the electro-optic coefficients for SBN. With this relatively high polarization anisotropy it becomes possible to linearly write the structure with typical beam power of few  $\mu\text{W}$  and without having significant feedback of the written structure onto the writing beam, but the probe beam experiences major refractive index modulation.

## 3. Paraxial wave equation and numerical methods

To study light propagation and soliton dynamics in nonlinear photonic lattices, we describe the dynamics of the optical field envelope  $A$  by the scaled paraxial wave equation

$$i \frac{\partial A}{\partial z} + \frac{1}{2} \nabla_{\perp}^2 A + \frac{1}{2} k_0^2 w_0^2 \Delta n^2(I) A = 0, \quad (1)$$

with  $\nabla_{\perp}^2 = \partial_x^2 + \partial_y^2$ . The transverse coordinates are scaled by a characteristic length  $w_0$  and the propagation distance is scaled by  $kw_0^2$  with  $k = 2\pi n/\lambda$ . The intensity-dependent index modulation  $\Delta n^2(I)$ , with  $I \propto |A|^2$ , accounts for the nonlinearity in this equation. In our system, this nonlinearity is caused by the photorefractive effect, that is well-described by the band transport model and the electro-optic effect that transfers an internal electric potential  $\phi$  into an index modulation  $\Delta n^2 = n_0^4 r_{\text{eff}} \partial_x \phi$ . Here,  $r_{\text{eff}}$  represents the effective electro-optic coefficient. The induction process of this internal potential can be approximated by the full anisotropic model [26]

$$\nabla^2 \phi + \nabla \ln(1+I) \cdot \nabla \phi = E_{\text{ext}} \frac{\partial}{\partial x} \ln(1+I) + \frac{k_B T}{e} \left( \nabla^2 \ln(1+I) + (\nabla \ln(1+I))^2 \right), \quad (2)$$

where  $E_{\text{ext}}$  is the external electric field that is applied along the crystal's c-axis. For moderate temperatures, drift in this external field dominates the transport of the photo-excited charge carriers and thus the whole induction process has an intrinsic orientation anisotropy caused by the directed transport.

We implemented spectral split-step beam propagation methods to simulate linear and nonlinear light propagation in the optically induced structures by evaluating the paraxial wave equation. In particular, we are interested in solitary solutions, thus we solve the wave equation with the ansatz  $A(r) = a(r_{\perp}) \exp(i\beta z)$ , where  $a(r_{\perp})$  is the transverse soliton profile and  $\beta$  denotes the propagation constant of the soliton. The resulting differential equation can be solved by using a modified Petviashvili iteration scheme [27].

## 4. Experimental results

### 4.1. Generation of modulated structures by superimposed Bessel beams

Figure 2 demonstrates several examples of nondiffracting beams resulting from the coherent superposition of two zero-order Bessel beams with varying transverse displacement and phase relation. The field distribution of the individual Bessel beams is given by  $E_{\text{Bessel}} \propto J_0(k_t \sqrt{(x-x_0)^2 + y^2})$ , where  $J_0$  represent the Bessel function of first kind,  $x_0$  the displacement from the origin, and  $g = \pi/k_t \approx 17.5 \mu\text{m}$  the generalized structure size. The distance  $d$  between the beam centers is measured in units of  $g$ .

The calculated and experimentally recorded intensity distributions for different separation distances between the Bessel beams are shown in Fig. 2. A whole variety of different structures can be addressed by simply changing the transverse displacement between the Bessel beams. For  $d = 1$ , as shown in Figs. 2(a), the structure shows similarities with a zero-order Mathieu beam [28], while for  $d = 1.5$  an azimuthally modulated quadrupole-like structure as in [14, 29] results, see Figs. 2(b). But here, the intensity ratio between the horizontal and vertical sites can additionally be tuned by slightly varying the distance  $d$ . Further increasing the distance  $d$  between the main lobes of the two Bessel beams, higher order Mathieu-like structures can be synthesized, cf. Figs. 2(c),(d). If a phase difference of  $\Delta\varphi = \pi$  between the beams is introduced, the corresponding field shows odd parity with respect to  $x$ , see Figs. 2(e).

In general, we should note that the arising structures share fascinating properties of the inter-

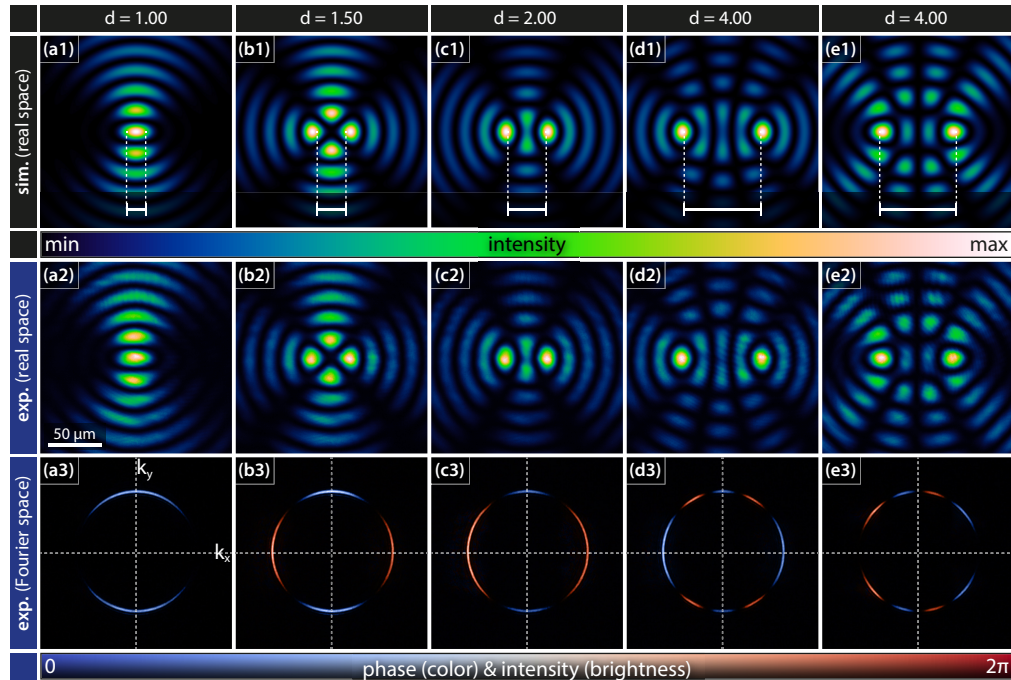


Fig. 2. Intensity patterns obtained by coherent superposition of two nondiffracting Bessel beams for different transverse displacement  $d$  (in units of Bessel structure size  $g$ ). (top row) Calculated intensity pattern, (middle row) experimentally recorded intensity profiles in real space. (bottom row) Experimentally recorded field distributions in Fourier space. The phase is encoded in the color, the brightness is given by the intensity. For (a)–(d) both Bessel beams are in phase, for (e) beams are  $\pi$  out of phase.

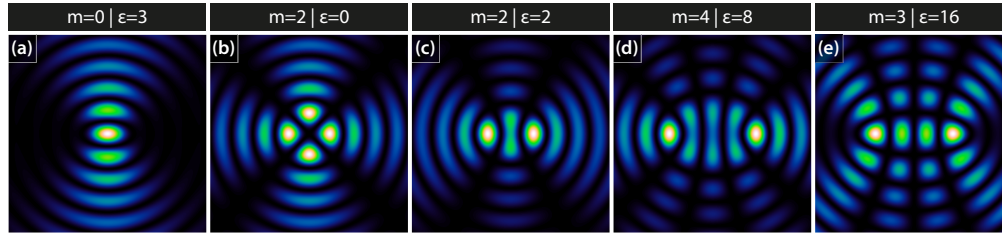


Fig. 3. Intensity distribution for Mathieu beams with different order  $m$  and ellipticity  $\epsilon$  that are almost identical to the resulting pattern in Fig. 2.

esting class of Mathieu beams that are solutions of the wave equation in an elliptical coordinate system [30]. According to the shape of the coordinate system, also the Mathieu beams exhibit elliptic symmetries and are determined by two quantities: the order  $m$  of the solution and the elliptic parameter  $\epsilon$  that reflects the separation between the two focal points of the ellipse. Figure 3 shows some numerically calculated Mathieu beams with different parameters  $m$  and  $\epsilon$  that are almost identical to the intensity profiles that resulted from the superimposed Bessel beams, cf. Fig. 2.

This quite simple approach of combining two zero-order Bessel beams already leads to a whole variety of intensity structures with geometries similar to Mathieu beams. Since the distance between the Bessel beams can be adjusted arbitrarily, the resulting geometries continuously transform into each other thus allow to create any intermediate state to be realized as writing beam for optical induction.

#### 4.2. Light guiding in focusing and defocusing regime

As one example, the quadruple-like structure [see Fig. 2(b)] is chosen representatively. After writing the azimuthally modulated index structure with an inner ring diameter (main lobe distance) of  $\varnothing \approx 34\mu\text{m}$  into the crystal, the next step was to study the light guiding capability for a propagating finite-size Gaussian beam (FWHM  $\approx 40\mu\text{m}$ ). Here, two different regimes are considered: focusing and defocusing. Focusing means, that the refractive index is locally increased

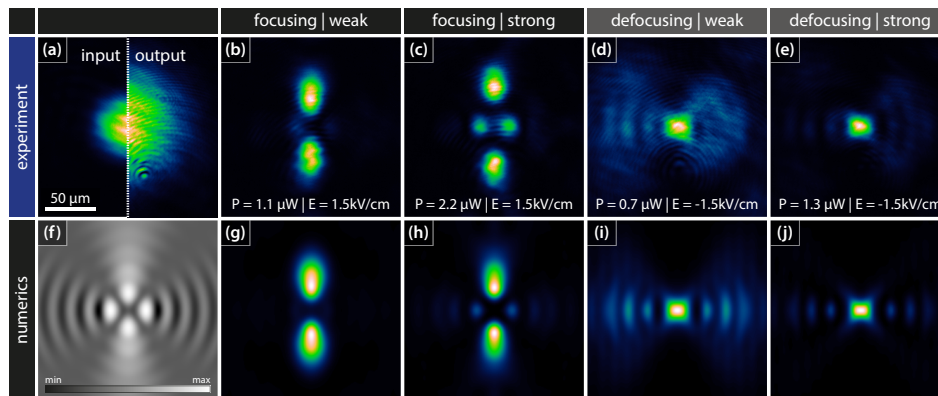


Fig. 4. Linear guiding and localization by 2d azimuthally modulated waveguide structure. (a) Input and output beam for homogenous crystal. (b),(c) Guided intensity at the output for a weakly induced focusing structure, (c),(h) for strong focusing structure. (d),(i) Guided intensity at the output for a weakly induced defocusing structure, (e),(j) for strong defocusing structure.

where the writing beam intensity is high and occurs if the external electric field is aligned along the *c*-axis of the crystal. If the field is applied anti-parallel to the *c*-axis, the photorefractive effect becomes defocusing – the index is locally decreased in high-intensity regions.

Figure 4 shows the experimental results, as well as the numerical simulations for the light-guiding structure probed with a Gaussian beam at the input face. This beam diffracts if no refractive index is written, as shown in Fig. 4(a). For weakly and strongly written focusing structures (depending on the writing time), see Figs. 4(b), 4(c), the intensity at the output nicely localizes at regions of locally increased index and consequently resembles the written refractive index structure that is shown in Fig. 4(f) (numerical simulation). These results indicate that the lattice potential is modulated stronger along the *c*-axis of the crystal [6, 12, 14].

The same measurement was performed in the defocusing case, where the refractive index is locally decreased in the high-intensity areas and the results are shown in Figs. 4(d) and 4(e). Here, the probe beam is localized in the center of the photonic structure where the writing beam has zero intensity and the refractive index of the crystal is larger compared with the illuminated areas where it is decreased. In this case the structure acts like a depressed cladding waveguide.

### 4.3. Soliton formation in modulated Bessel-like photonic lattices

Finally, we demonstrate spatial soliton formation inside this particular quadrupole-like waveguide structure. In contrast to previous studies where more complex compound solitons in this azimuthally Bessel lattices were investigated [18], we here want to restrict ourselves to the fundamental case of a bright soliton in one particular lobe of the structure. In a first step, the stable soliton solution of the paraxial wave equation is numerically calculated and the resulting field distribution is realized experimentally and imaged onto the input face of the crystal, see Fig. 5(a). Here, we use SLM 2 to precisely shape the probe beam to match the soliton profile. To minimize the distortion caused by the inherent anisotropy of the index modulation, the soliton is settled on one of the horizontal sites, see Fig. 5(b).

The formation of the soliton is demonstrated by the transition from linear waveguiding to nonlinear localization by increasing the probe beam power, see Figs. 5(c)–5(e). In the linear

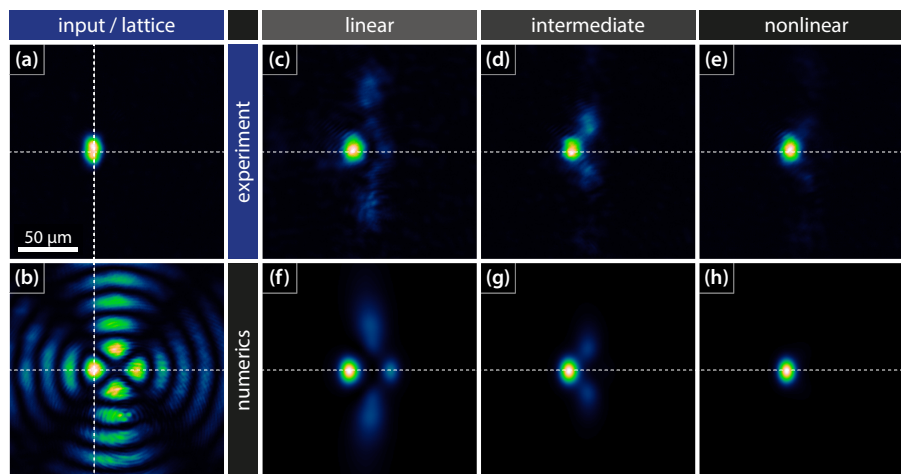


Fig. 5. Nonlinear off-center soliton formation in azimuthally modulated Bessel-like structure. (a) Experimentally realized probe beam at the input (soliton profile is calculated numerically) and (b) induction beam. (c)–(e) Experimentally observed soliton formation for increasing probe beam intensity. (f)–(h) Corresponding numerical simulations.

regime, Fig. 5(c) (where the probe beam is switched off during writing), the launched localized soliton profile diffracts since the confining nonlinear refractive index modification is missing. Increasing the probe beam power to half of the necessary power, Fig. 5(d) ( $P_p \approx 20\text{ nW}$ ), the intensity still leaks out to the neighboring sites of the structure. For the ideal probe beam power  $P_p \approx 41\text{ nW}$  [Fig. 5(e)], the soliton is formed and the intensity profile at the output looks identical to that at the input. Moreover, the experimental observations meet the numerical results [Fig. 5(bottom row)].

## Conclusion

In conclusion, we have presented a powerful approach to realize a huge variety of nondiffracting light fields by coherent superposition of two co-propagating zero-order Bessel beams. The resulting transverse structures depend on the distance and the phase relation between the Bessel beams and can be continuously transformed to mimic several Mathieu beams of different order and parity. We demonstrated the optical induction of one representative quadrupole-like structure and investigated the linear light guiding behavior in the focusing and defocusing regime. Finally, we presented the formation of stable spatial solitons in this structure. Our obtained results can be used for construction of all-optical photonic interconnects.

## Acknowledgments

This work was supported by bilateral collaborative German-Armenian Project financed by State Committee of Science Armenia (Project no. HG-02) and German Federal Ministry of Education and Research (Project no. WTZ-ARM-2012-006)